

111-20125662 Analysis of Combustion Process in a Diesel Engine with Multi-Stage Injection Using a Stochastic Combustion Model

Long Liu¹⁾ Naoto Horibe²⁾ Takuji Ishiyama³⁾

*1) 2) 3) Kyoto University, Graduate School of Energy Science
Yoshida-honmachi, Sakyo-ku, Kyoto, 606-8501, Japan (E-mail: liulong210@gmail.com)*

Presented at the JSAE Annual Congress on Oct., 3 ,2012

ABSTRACT: In order to carry out parameter studies on multi-stage injection, a phenomenological model has been constructed. This model was based on a stochastic ignition/combustion model and included calculations of air entrainment, turbulence mixing, chemical reaction and interaction between the sprays from different injection stages. The model was validated against experimental data from a single cylinder test engine. And then, analysis was performed based on the microscopic information of entrained air, fuel-air mixing, and the progress of chemical reactions under different injection conditions to understand the mechanisms of combustion with multi-stage injection.

Key Words: (Standardized) heat engine, compression ignition engine, combustion analysis (Free) Diesel engine simulation, Multi- stage Injection, Stochastic combustion model (A1)

1. INTRODUCTION

Among various technologies applied to improve the thermal efficiency and alleviate the pollution for diesel engines, the injection control has played a significant role, especially the multi-stage injection is essential for the latest engines to reduce NOx, soot emissions and combustion noise. There are many injection parameters such as injection pressure, timing and quantity, and these parameters should be selected properly corresponding to the engine operating conditions. To obtain the strategies for the selection, the change in combustion process when varying these parameters is necessary to be understood more deeply.

For this purpose, a phenomenological model has been developed based on the stochastic combustion model⁽¹⁾⁽²⁾ with modifications including spray penetration, air entrainment rate, interaction between the spray from sequent injection stages for combustion calculation with multi-stage injection. The simulation results were compared with experimental data from a single cylinder test engine for pilot/main two-stage injection. And then the heat release rate and the microscopic information inside the spray, such as probability density function (PDF) of equivalence ratio, were analyzed to optimize the model.

2. MODEL DESCRIPTION

2.1. Model's concept

In this model, the volume in the cylinder is divided into three zones to represent the sprays and ambient gas for two-stage injection situation, including the first spray zone, the second spray zone and the ambient air zone. And the fuel

evaporation, turbulence mixing, and chemical reaction are calculated in the each spray zone respectively, meanwhile the entrainment mechanism is applied to describe the mass and heat transfer among these three zones. The specific process is as follows.

Before injection, the air and EGR gas in the cylinder is treated as ambient air zone that is presumed to be composed of a great number of fluid elements. Then after the start of the first injection, the fuel is injected into the cylinder as fluid elements, and entrained fluid elements from ambient air zone to form the first spray zone. After the end of the injection, the first spray tail is assumed to depart from nozzle exit to the downstream. When the second injection starts, the first and second spray zone exist in the cylinder and the fluid elements of ambient air zone are entrained into these two spray zones respectively. Once the second spray tip overtakes the first spray tail, both of the fluid elements from the ambient air zone and the first spray zone are entrained into the second spray zone. Finally these two spray zones are combined into one spray zone after all of the fluid elements of the first spray zone are entrained into the second spray zone.

2.2. Spray penetration and entrainment rate

Obviously, the spray tip and tail penetration and air entrainment rate are primary parts to carry out the model's concept, especially after the end of injection (EOI). However, there are very few studies on the spray characteristics after EOI. Here, the zero-dimensional model was developed based on the Musculus's transient jet model⁽³⁾.

2.2.1. Spray tip penetration and air entrainment rate

To realize the calculation of spray tip penetration and air entrainment rate after EOI, the entrainment wave theory is employed in our model. Entrainment wave theory was proposed by Musculus⁽³⁾ to describe the turbulent jets penetration and entrainment evolution in decelerating transient, and this theory was also used to analyze diesel jets based on a one-dimensional discrete model successfully⁽⁴⁾. Thus the modeling method of this one-dimensional discrete model is only used for the treatment of the spray tip part, so that the spray tip penetration and air entrainment rate can be derived for zero-dimensional calculation in this study.

2.2.2. Spray tail penetration

After EOI, the mixture near the nozzle becomes very lean because the fuel supply is terminated. Therefore, it is assumed that the part of the spray near the nozzle acts as ambient air zone and a spray tail exists. The tail position is determined so that 10% of total fuel is contained in a region from the nozzle to the tail.

2.3. Interaction between the sprays from sequent injection stages

The interaction between the sprays from sequent injection stages is caused by the entrainment of the second spray from the first spray after the arrival of the second spray tip at the first spray tail. To mimic this interaction, it is requisite to obtain the amount of the first spray mixture entrained into the second spray.

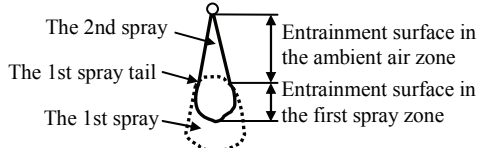


Fig. 1 Spray interaction diagram

Indeed, the entrainment behavior can be considered as that the spray entrains the ambient gas through the spray boundary that is a conical surface, therefore the entrainment rate can be represent as the product of air density, entrainment velocity over the spray boundary surface and area of spray boundary surface. After the second spray tip touches the first spray tail, the entrainment area of the second spray is divided into two parts by the first spray tail as shown in Fig 1. The ratio of the entrainment rate of these two parts (R_e) can be obtained as equation (1) with assumptions as the air and the first spray have the same density and the entrainment velocity uniformly distribute over the spray boundary surface in the ambient air zone and the first spray zone respectively.

$$R_e = C_e \frac{A_{\text{air}}}{A_{\text{spray}}}, \quad (1)$$

where A_{air} and A_{spray} is the area of the spray boundary surface in the ambient air zone and the first spray zone respectively. C_e is a coefficient given to describe the difference between the entrainment velocity over the spray boundary surface in the ambient air zone and the first spray zone. Based on equation (1) and the total entrainment rate of the second spray, it is able to obtain the amount of the first spray mixture entrained into the second spray.

3. RESULTS AND DISCUSSION

Based on the modifications above, calculations were performed simulating a single-cylinder diesel test engine with two-stage injection. The specifications of test engine are listed in Table 1, and the calculation conditions are listed in Table 2.

Table 1 Standard specifications of test engine

Engine type	Single-cylinder, DI-Diesel engine
Bore × Stroke	85×96.9 mm
Displacement	550 cc
Compression ratio	16.3
Combustion chamber	Reentrant type ($\phi 51.6$ cavity)
Injection system	Common-rail system 0.125 mm × 7 holes nozzle

Table 2 Simulation performing conditions

Injection pressure	125MPa
Total injection quantity	32mm ³
Pilot injection quantity	2, 4, 6mm ³
Pilot injection timing	-9, -19, -24° ATDC
Main injection timing	1° ATDC
EGR ratio	20%
Swirl ratio	2.0

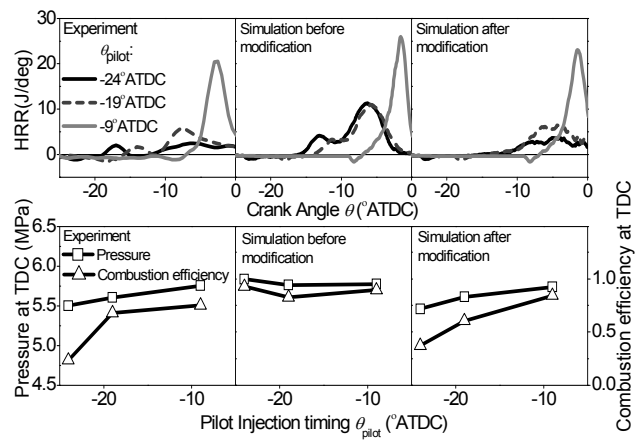


Fig. 2 Effects of pilot injection timing on pilot spray's heat release rate, pressure and combustion efficiency at TDC

$$(q_{\text{pilot}}=2\text{mm}^3)$$

3.1. Heat release rate of pilot spray

Figure 2 shows the effects of pilot injection timing on the heat release rates of pilot spray, pressure and combustion efficiency of pilot fuel at TDC for injection quantity of 2mm^3 . From the experimental data (left), it can be found that the total released heat of pilot spray increases as the pilot injection is retarded. However the simulation results (center) reveal almost the same value of total released heat. This difference is assumed to be mainly caused by slow heat release from the mixture in squish region. The early injection timing makes the spray flow into the squish region and impinge on the cylinder liner or piston top. Due to the low temperature of the walls and/or the adherence of fuel on the piston top surface, oxidation reaction and mixing in the mixture are attenuated. Thus the earlier pilot injection timing obtains the lower heat release.

To mimic such effects, the volume ratio of the spray flowed into squish and total spray is considered as a factor reducing the mixing rate. As shown in Fig.3, if the spray tip cross-sectional area impinges on the bowl lip edge, the incremental volume of the spray can be divided into two parts, squish part and bowl part. Thus the volume ratio between squish part and incremental spray ($R_{\text{sq,inc}}$) can be calculated as

$$R_{\text{sq,inc}} = \frac{C(\theta)A_{\text{up}}}{C(\theta)A_{\text{up}} + A_{\text{bl}}} , \quad (2)$$

where A_{up} and A_{bl} is the area of the cross-sectional area at impinging timing over and below the bowl lip edge respectively, and the $C(\theta)$ is a function of the angle between the spray central line and cylinder head, and it is used to describe the difference of spray spreading velocity in squish region and bowl region. This function is selected as $\cot \theta$ in this study. Sequentially, the volume ratio of spray flowed into squish region and total spray (R_{sq}) can be obtained as

$$R_{\text{sq}} = \frac{\int_{t_{\text{im}}}^t R_{\text{sq,inc}} \dot{V}_{\text{spray}} dt}{V_{\text{spray}}} , \quad (3)$$

where t_{im} is the impinging timing and V_{spray} is the total spray volume.

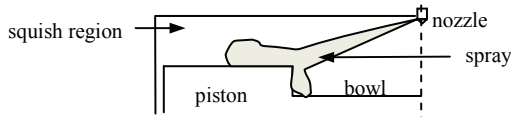


Fig. 3 Wall impingement diagram

And the stochastic collision frequency (ω) is represented as follows,

$$\omega = \omega_0 (1 - C_m R_{\text{sq}} G_j^{-0.2}) , \quad (4)$$

where C_m is a constant, ω_0 is the collision frequency of free spray, and G_j is the total turbulence energy generated by

injection, which is used to weaken the R_{sq} effect on mixing, because the larger turbulence energy generated by injection causes the stronger mixing.

After this modification, the simulation results in Fig.2 (right) reveal the trends similar to those in experimental data.

3.2. Heat release rate after main injection

After the above modification, calculations were performed for combustion with pilot/main two-stage injection. The results of heat release rate are shown in Fig.4 (middle). The ignition timings are well predicted, however, the second peaks of heat release rates after main injection are lower and later than those of experiments. Combined with the PDF history of equivalence ratio in Fig.5 (left), it can be found that most of the elements has been ignited at 8°ATDC , so that the combustion hereafter is controlled by the mixing rate. Before 12°ATDC , the main spray entrains air and the pilot spray mixture together, thereby the air entrainment rate is at a low level, and it leads to slow formation of combustible mixture, which is indicated as a lower peak of PDF in lean side. Therefore the heat release rate increases slowly. After 12°ATDC , all of the pilot spray is entrained into the main spray, the air entrainment rate raises up, and the heat release rate increases faster.

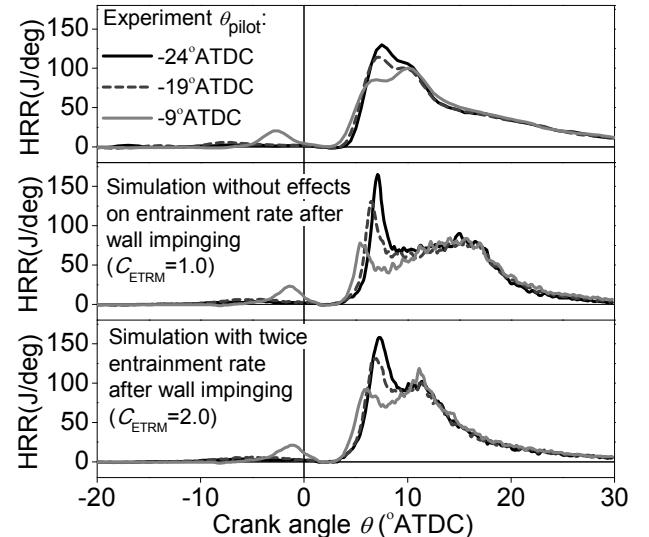


Fig. 4 Effects of pilot injection timing on heat release rate ($q_{\text{pilot}}=2\text{mm}^3$)

Based on this analysis, the effect on air entrainment by spray wall impingement was included in the model. It is reasonable to consider the enhancement of air entrainment at least in the initial stage of wall impingement (around 3°ATDC). Thus a constant (C_{ETRM}) is given to multiply the air entrainment rate of free spray after the wall impinging. The results with twice entrainment rate after wall impinging ($C_{\text{ETRM}}=2.0$) is showed in Fig.4 (bottom). The second peaks behavior is

improved and the entire heat release rates obtain similar curves with experiment. At the same time, its PDF history of equivalence ratio in Fig.5 (right) shows the faster mixing rate than that without enhancing the entrainment rate.

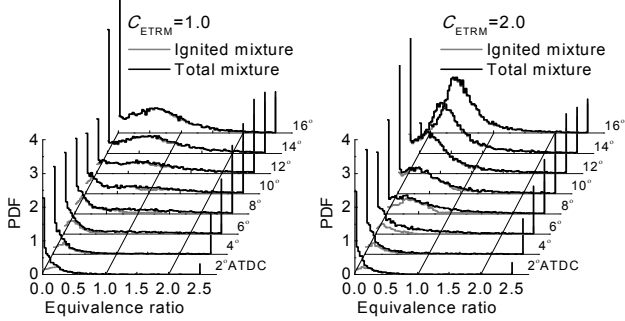


Fig. 5 Histories of PDF for equivalence ratio
($q_{\text{pilot}}=2\text{mm}^3$, $\theta_{\text{pilot}}=-19^\circ\text{ATDC}$)

3.3. Heat release rate during late combustion period

Another discrepancy between calculation and measurement is found in the later part of heat release rate. The calculated heat release rate decreases more rapidly than in measurement as shown in Fig.4. This is because the ambient air is consumed completely too early in the calculation. Thus the entrainment rate should be decreased in the later part of combustion to reproduce the measured tendency. In fact, because of the neighbour sprays interaction, the air entrainment area of the spray is decreased with the spray volume increasing, and it reduces the air entrainment rate. This influence is considered in a simple way as follows,

$$\dot{m}_e = \dot{m}_{e0} \left(1 - C_{vr} \frac{V_{\text{spray}} \times n_{\text{hole}}}{V_{\text{cyl}}}\right), \quad (5)$$

where \dot{m}_e is the air entrainment rate affected by spray-volume increase, \dot{m}_{e0} is the original air entrainment rate, n_{hole} is the number of nozzle holes, V_{cyl} is the volume in cylinder, and C_{vr} is a constant to fit the experiment data. Considering that the suppression of air entrainment due to this mechanism would be prominent after the end of injection, the equation (6) is applied after the transition timing⁽³⁾ when the entrainment wave arrives at the spray tip, because the entrainment rate of free spray starts to decrease after this timing. In addition, the entrainment wave starts from the injection speed deceleration, and twice of the duration from the start of injection to entrainment wave start timing is the transition time. Thus the transition timing (t_{tr}) is decided as

$$t_{tr} = 2C_{EW} t_j, \quad (6)$$

where t_j is the injection duration, and C_{EW} is a constant with the value from 0 to 1.

Finally, the model constants are selected as $C_{ETRM}=1.5$, $C_{vr}=0.8$, and $C_{EW}=0.52$. The results are shown in Fig.6. It

reveals that the model can obtain the similar heat release rate shape for each case, and it also can capture the same tendencies of the heat release rate with the pilot injection timing and injection quantity changing.

4. CONCLUSION

In this paper, the spray penetration, air entrainment rate, interaction between the spray from sequent injection stages were studied and modeled to modify the stochastic combustion model to realize the calculation of multi-stage injection situations. And then the mixing rate and air entrainment rate were optimized for simulation of pilot/main two-stage injection, based on the analysis of combustion process. The results reveal that the model has capability to accurately predict the ignition and combustion characteristics of diesel engine with pilot/main two-stage injection. In addition, the NOx and soot calculation and simulation for multi-stage injection cases will be carried out in the future.

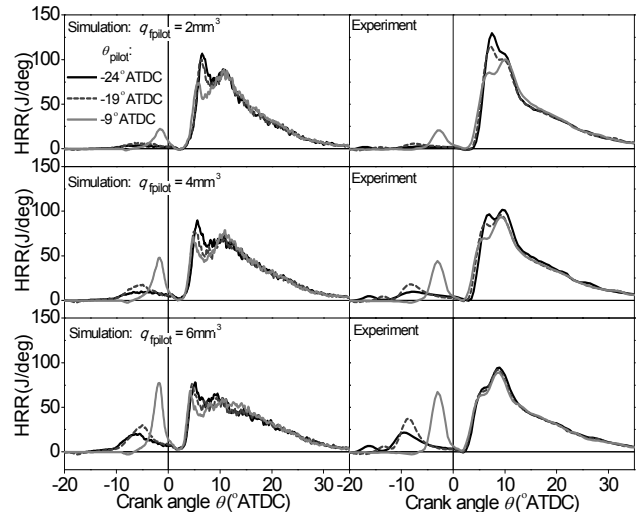


Fig. 6 Effects of pilot injection timing and injection quantity on the heat release rate

REFERENCES

- (1) M. Ikegami: A Stochastic Approach to Model the Combustion Process in Direct-Injection Diesel Engines, Twentieth Symp. (Int.) on Combustion, p.217-224 (1984).
- (2) T. Ishiyama: Modeling and Experiment of NOx Formation in DI-PCCI Combustion, SAE Paper 2007-01-0194 (2007).
- (3) Mark P. B. Musculus: Entrainment Waves in Decelerating Transient Turbulent Jets, J. Fluid Mech., Vol. 638, p.117-140 (2009).
- (4) Mark P. B. Musculus: Entrainment Waves in Diesel Jets, SAE Paper 2009-01-1355 (2009).